# Symbitron Exoskeleton: Design, Control, and Evaluation of a Modular Exoskeleton for Incomplete and Complete Spinal Cord Injured Individuals

C. Meijneke [ID], G. van Oort [ID], V. Sluiter, E. van Asseldonk [ID], N. L. Tagliamonte, F. Tamburella [ID],
I. Pisotta [ID], M. Masciullo [ID], M. Arquilla, M. Molinari [ID], A. R. Wu [ID], F. Dzeladini,
A. J. Ijspeert [ID], *Fellow, IEEE*, and H. van der Kooij

*Abstract*— In this paper, we present the design, control, and preliminary evaluation of the Symbitron exoskeleton, a lower limb modular exoskeleton developed for people with a spinal cord injury. The mechanical and electrical configuration and the controller can be personalized to accommodate differences in impairments among individuals with spinal cord injuries (SCI). In hardware, this personalization is accomplished by a modular approach that allows the reconfiguration of a lower-limb exoskeleton with ultimately eight powered series actuated (SEA) joints and high fidelity torque control. For SCI individuals with an incomplete lesion and sufficient hip control, we applied a trajectory-free neuromuscular control (NMC) strategy and used the exoskeleton in the ankle-knee configuration. For complete SCI individuals, we used a combination of a NMC and an impedance based trajectory tracking strategy with the exoskeleton in the ankle-knee-hip configuration. Results of a preliminary evaluation of the developed hardware and software showed that SCI individuals with an incomplete lesion could naturally vary their walking speed and step length and walked faster compared to walking without the device. SCI individuals with a complete lesion, who could not walk without support, were able to walk with the device and with the support of crutches that included a push-button for step initiationOur results demonstrate that an exoskeleton with modular hardware and control allows SCI individuals with limited or no lower limb function to receive tailored support and regain mobility.

*Index Terms*—Exoskeleton, modular, orthosis, SCI, series elastic actuation (SEA), neuromuscular control (NMC).

## I. INTRODUCTION

INDIVIDUALS with spinal cord injuries (SCI) experience reduced or complete loss of mobility, but wearable technologies such as lower-limb exoskeletons could be used to assist gait and help improve their quality of life. Several commercially available exoskeletons have been developed for and used by subjects with a complete SCI [1]. They mostly consist of a structure that allows actuation of knee and hip flexion and extension movements. The exoskeleton joints are typically controlled in a position control mode, where the motions of the human joints are enforced and cannot be influenced by the user. However, about 60% of individuals who have suffered a spinal cord injury only have an incomplete lesion and have some remaining function in their lower extremities [2]. The remaining movement capabilities depend on the severity and location of the lesion; the lower (the more inferior/caudal) the lesion, the more remaining function in the lower leg joints starting from the most proximal joints (the hip) to more distal joints [3]. Exoskeletons also have great potential to improve the walking ability of individuals with a incomplete lesion (in terms of speed, endurance and stability) if they can substitute for the lost or impaired function and leave control of the unaffected joints to the individual. This approach requires a different class of exoskeletons that can be tailored to the individual's needs and provides assisting forces without enforcing movements.

Traditionally, exoskeletons are controlled using predefined trajectories, which has resulted in reliable support of people with a complete lesion during walking over flat ground. However, predefined trajectories are inflexible when it comes to adapting to varied terrain (e.g., uneven sidewalks, unpaved

Fig. 1. SCI test pilots using the modular exoskeleton in knee-ankle configuration (KA) on the left and hip-knee-ankle configuration (HKA) on the right.

**TABLE I**
PART OF THE USE CASES TABLE FOR THE EXOSKELETON. PRIORITY IS INDICATED BY M: MANDATORY, D: DESIRED; OR O: OPTIONAL. ACHIEVEMENTS IS INDICATED BY IL: ACHIEVED BY SCI PILOTS WITH INCOMPLETE LESION, CL: ACHIEVED BY SCI PILOTS WITH COMPLETE LESION

| Use Case | Priority | Achieved |
|---|---|---|
| **Donning and Doffing** | | |
| With help of another person | M | IL + CL |
| by him/herself | D | IL |
| **Sit-to-stand and Stand-to-sit (STS)** | | |
| With support of own arms or external support | M | IL + CL |
| **Standing / maintain balance** | | |
| Maintain balance when undisturbed | M | IL + CL |
| … while performing activities of daily life (ADL) using arms | D | IL |
| **Free walking** | | |
| Initiate walking with the help of another person | M | IL + CL |
| Initiate walking by him/herself | D | IL + CL |
| Walk in straight line on level ground, 0.5 m/s (W0.5) | M | IL + CL |
| Walk in straight line on level ground, 0.8 m/s (W0.8) | D | IL |
| Walk in curve on level ground | D | IL + CL |
| Turn | D | IL + CL |
| Side-stepping | D | IL |
| Stop walking with the help of another person | M | IL + CL |
| Stop walking by him/herself | D | IL + CL |
| Walk up and down a slope with the help of another person | M | IL + CL |
| Walk up and down a slope by him/herself (SLP) | D | IL + CL |
| Walk at different speeds | M | IL + CL |
| Change speed during walking | D | IL |
| Resist small disturbances (involuntary shift of center of mass) | D | IL |
| Avoid obstacles | O | IL |
| Walk on uneven terrain | O | IL + CL |
| **Stair ascending and descending (STR)** | | |
| With the help of hand rails or another person | D | IL + CL |
| Without external support | O | IL + CL |

roads, slopes) and walking speed. Also, for people with some remaining walking capabilities, control would ideally be shared between the person and the exoskeleton. The reflex-based musculoskeletal model proposed by Geyer and colleagues [4], [5] has the potential to tackle both problems. In this model, joint torques are generated by local reflex loops in such a way that natural gait emerges. The local reflex loops react to changes in leg motion, for example to deviations due to uneven terrain, or when the person voluntarily initiates movement by using their remaining motor function. Previously we have incorporated these models as controllers (called neuromuscular controllers, *NMC*) for a powered ankle exoskeleton [6]. In a follow up study, we demonstrated with this wearable Achilles ankle exoskeleton that incomplete SCI individuals improved their walking speed and step length wearing the device over different training sessions, and we also found an unexpected increased walking speed using no device after a brief training period with the exoskeleton [7]. NMC controllers for the knee and hips were also rendered on the haptic robotic gait trainer LOPES II [8], where we showed the first application of NMC controllers on a lower limb exoskeleton.

We aimed to develop a personalizable Wearable Exoskeleton that enables individuals with incomplete or complete SCI to walk again. The exoskeleton consisted of a set of powered modules, one for each lower limb joint. Personalization was accomplished by selecting only those joint modules required to compensate for the loss of function for that specific person and tailoring the control and human-machine interface. This paper encloses for the first time the full details about the mechanical and electrical hardware and on the low level control of the modular Symbitron exoskeleton, in addition to CAD drawings of the ankle and knee modules that were disclosed before [9]. We also show for the first time that walking speed in incomplete SCI individuals can be increased with a wearable ankle-knee exoskeleton utilising a biological inspired neuromuscular control approach.

In this paper, we describe the use cases and requirements for the exoskeleton (section II), the mechatronic design (section III), and the low-level and high-level control (section IV). The device was preliminary evaluated for SCI individuals with a complete or with an incomplete lesion (section V). Analogous to those who control prototypes of airplanes or race cars, we prefer to call our exoskeleton users *SCI test pilots* instead of 'individuals' or 'patients' and will use this term in the remainder of the paper.

## II. REQUIREMENTS

Before starting the design process, the requirements for the device were specified. First, *use cases* were specified and structured (Table I). Requirements were all rated according to priority:

**M** Mandatory (essential to function of the device),
**D** Desired (will be aimed for in the design but should not hinder achieving the mandatory requirements),
**O** Optional (would be nice to have, but no great effort will be done to achieve it).

The table was created from a discussion among clinicians, researchers, and engineers that were involved in development of the exoskeleton. The aim of this discussion was to find a compromise between what is most important for our SCI test pilots, exceeds or matches the state-of-the-art, and is technically achievable.

TABLE II

Data, Including Speed in Rpm, Torque in Nm, Power in W, and Range of Motion (Rom) Deg, for Various Use Cases From Table I. Based on a Maximum Body Mass of Our SCI Pilots of 85 Kg and a Height of 1.8 m. The Dotted Values Are Not Reported in the Source

| | | STS [10], [11]¹ | W0.5 [12], [13]² | W0.8 | SLP [14]¹³ | STR [15]¹ |
|---|---|---|---|---|---|---|
| Speed (rpm) | ADP | 6.5 | 13.4 | 22.0 | ... | ... |
| | KFE | 21.9 | 24.8 | 32.5 | ... | ... |
| | HFE | 22.0 | 13.4 | 19.1 | ... | ... |
| | HAA | ... | 1.1 | 1.2 | ... | ... |
| Moment (Nm) | ADP | 65.5 | 119.0 | 129.2 | 202.3 | 123.3 |
| | KFE | 102.9 | 37.4 | 40.0 | 158.1 | 113.9 |
| | HFE | 73.1 | 36.6 | 49.3 | 112.2 | 74.0 |
| | HAA | ... | ... | ... | ... | 109.7 |
| Power (W) | ADP | ... | 72.3 | 172.6 | ... | 303.5 |
| | KFE | ... | 22.1 | 60.4 | ... | 237.2 |
| | HFE | ... | 31.4 | 73.1 | ... | 167.5 |
| | HAA | ... | ... | ... | ... | 101.2 |
| Rom (Deg) | ADP | 0.0 | 10.9 | 10.9 | 42.9 | 21.2 |
| | | 31.3 | 13.8 | 13.8 | 14.4 | 35.5 |
| | KFE | 111.2 | 63.0 | 63.0 | 76.2 | 99.1 |
| | | 0.0 | 4.0 | 4.0 | 0.0 | 0.0 |
| | HFE | 107.7 | 28.1 | 28.1 | 57.1 | 71.0 |
| | | 0.0 | 12.0 | 12.0 | 22.5 | 0.0 |
| | HAA | ... | 20.1 | 20.1 | ... | 12.6 |
| | | ... | 14.9 | 14.9 | ... | 20.6 |

¹maximum of the mean including two standard deviations ²peak value ³Based on a grade of 15%

From the use cases combined with various data sources, a table with maximum velocity, torque and power was compiled (see Table II). Note that every use case sets additional design constraints for the system

## III. Modular Hardware Design

### A. Overview

The exoskeleton has 8 powered joints and 4 passive joints (Figure 2). Some parts of the exoskeleton can be electrically and mechanically disconnected from the others and controlled independently. Due to the position of the attachments to the user (cuffs, belts, etc.), the following configurations are possible:

- Ankle (A configuration),
- Knee-ankle (KA configuration),
- Hip-knee-ankle (HKA configuration),
- Hip (H configuration).

Each configuration can be used for one leg or for both legs. .

The backpack module is always needed because it contains the control computer, power management, and batteries. When the hip module is not used, it is worn as a normal backpack that is not mechanically attached to the knee or ankle modules. Each powered joint contains a custom designed series elastic actuator (SEA) unit that will be discussed in more detail in the next section. Table III shows the mass of the exoskeleton and its sub-assemblies.

### B. The Series Elastic Actuator (SEA)

All actuated joints of the exoskeleton are powered by a rotary series elastic actuator. The actuator consists of a
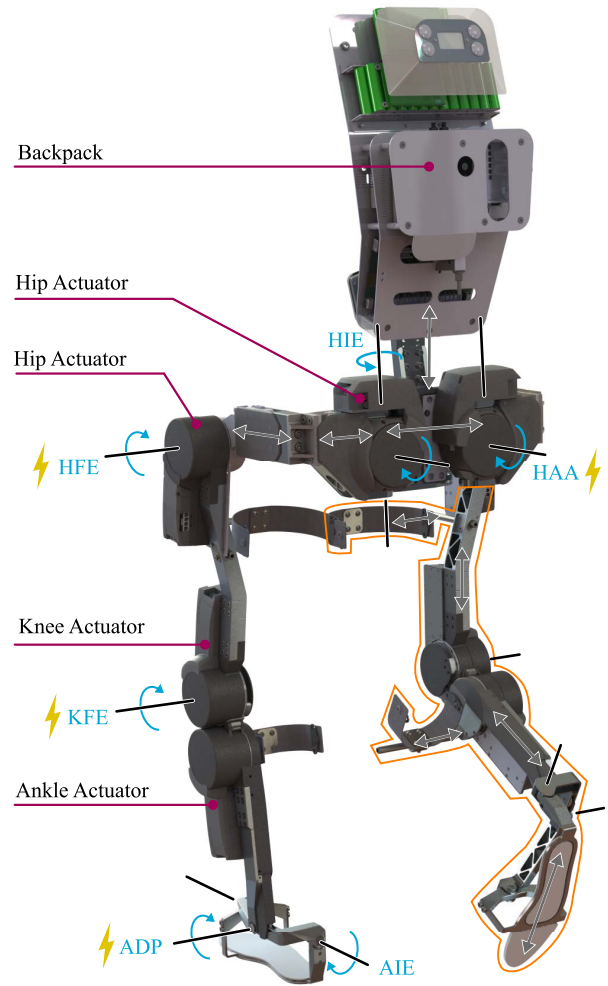


Fig. 2. Rendered CAD-model of the Symbitron exoskeleton showing the joints hip abduction and adduction (HAA), hip internal and external rotation (HIE), hip flexion and extension (HFE), knee flexion and extension (KFE), ankle dorsiflexion and plantarflexion (ADP), and ankle inversion and eversion (AIE). The joints with an electricity icon are powered by a SEA and the joints without are passive. The HIE joint is loaded with an adjustable spring and can be locked. The AIE joint can be free or locked. This picture shows the hip-knee-ankle (HKA) configuration. The orange region indicates the right leg Knee-ankle (KA) configuration. The straight grey arrows show the size adjustments available on the exoskeleton.

TABLE III

Measured Mass of the Exoskeleton Components

| Components | Mass per leg kg | Total mass kg |
|---|---|---|
| Backpack incl. batteries | - | 8.0 |
| Back Plate incl. pelvis and shoulder straps | - | 3.1 |
| HAA Actuator and hip structure | 3.9 | 7.7 |
| HFE Actuator and connector plate | 2.2 | 4.3 |
| KFE Actuator, thigh structure and cuff | 3.2 | 6.4 |
| ADP actuator, shank structure and cuff (excl. shoe) | 3.8 | 7.7 |
| **Total mass** | **13.0** | **37.2** |
| Total Actuator mass | 6.4 | 12.8 |

cylindrical housing with an envelope $\phi 100 \times 70$ mm. The main components are:

- *Brushless Motor (Tiger-Motor U8 PRO 170Kv).* The maximum continuous output power is 520 W.

- *Strain wave gear (Leader drive, LCSG-20)*. In HKA configuration, all ratios are chosen to be 100, except the knee, which is 50. The peak torque and speed are 102 Nm and 3.14 rad/s for gear ratio 100, and 69 Nm and 6.28 rad/s for ratio 50, respectively.
- *Custom design titanium spring*. The spring can be loaded up to 120 Nm with a life of $10^7$ cycles (these specification were obtained from finite element analysis) and has a spring constant of 1500 Nm/rad.
- *Cross-roller bearing (THK, RA 7008)*. It supports the output rotation including the external and internal moments in all directions.
- *Three absolute encoders*. These encoders measure the joint output angle, spring deflection ($2 \times$ RLS Aksim 20 bits BiSS), and motor angle (IC-Haus MHM 14 bits BiSS).

To implement the actuator basis in a joint, the drive electronics can be oriented and positioned in the most suitable way, and the housing and output flange are manufactured with the desired connections to the surrounding parts. The weight of one actuator including electronics is 1.6 kg. The drive electronics for each drive consist of a motor drive with EtherCAT interface (Technosoft, iMOTIONCUBE). A custom EtherCAT slave was developed to read the joint and spring deflection encoders, temperature, and an Xsens Inertia Measurement Unit (IMU).

### C. The Structure

The main goal of the exoskeleton structure is to connect the actuators to each other and to the human body in such a way that the actuator's torque (and external forces) are conveyed to the wearer in a safe and stable manner. In addition, the structure facilitates joint-to-joint routing of power and communication cables. This means that the actuator rotation center has to coincide with the human joint center as much as possible. An important constraint for the design of the structure is to keep the exoskeleton close the body to ensure that there is minimal interference with the wearer or environment. As SCI test pilots have different body sizes and shapes, the exoskeleton structure needs the ability to be resized to each individual pilot.

The exoskeleton can be tailored to a SCI test pilot by changing 23 settings (see Figure 2). Most of the components (such as the bars connecting the knee joint and ankle joint) are manufactured in multiple sizes and can be interchanged to change the size of the exoskeleton. This approach was chosen to reduce weight by omitting telescopic mechanisms and to create a truly personalized exoskeleton.

### D. The Backpack

The electrical components that are not needed on the leg are placed in the backpack. The description of its contents and the design choices made are described below.

Two Li-ion batteries (Energus; Vilnius, Lithuania) with a total mass of 2.5 kg are situated in the backpack: one 7S2P for the logic power and one 13S3P for the motor power. Interestingly, operation time is entirely limited by the logic battery. The power-hungry EtherCAT slaves together with the internal PC and all other electronics drain the logic battery in about one hour. In contrast, the motor battery usually lasts for a multitude of that.

A custom PCB inside the backpack was developed to be able to switch motor and logic power on or off, and to provide an extra guard over the battery voltage. This board also provides: (1) DC power to the PC, EtherCAT splitter , and IMU interface, and (2) an interface to the emergency stop button. When the emergency button is pressed, all motor drives are disabled, and the motor battery is switched off.

Computational power is provided by a small PC (Intel NUC5i5RYH). The communication protocol used in the exoskeleton is EtherCAT.

Because the purpose of the exoskeleton was enabling experiments using novel control strategies, it is likely that interfaces to additional devices are required. Therefore there is room within the backpack for additional EtherCAT slaves. Several of these were made, and used in different combinations throughout the experiments:

- *IMU box*. This is an interface between the Xbus master of Xsens (Xsens, Enschede, the Netherlands) and EtherCAT. This device makes the quaternion data of 3 IMUs available on the EtherCAT bus.
- *Crutch interface*. Two buttons were integrated in the handle of a crutch to initiate steps in experiments with the HKA configuration. An EtherCAT slave was made to read those buttons.

Apart from the backpack and the actuator electronics, a small PCB was designed to read the pressure insoles (IEE; Contern, Luxembourg) and determine heel and toe contact with the ground.

## IV. CONTROLLER DESIGN

The control PC, situated in the backpack, runs Windows 7. For the EtherCAT master software, TwinCAT 3.1 was chosen to allow detailed diagnosis of low-level EtherCAT communication without having to implement additional diagnostics software. The controllers were developed in Simulink (2015b, Matlab, Mathworks). The Simulink models were compiled for real-time usage in TwinCAT. Simulink itself is used as GUI by running it in 'external mode'. The model runs at 1000 Hz.

The control can be separated into two hierarchical levels: low-level and high-level control, which are described separately below.

### A. Low-Level Joint Control

Low-level control refers to the control of individual joints to ensure that each joint generates the desired torque on its output shaft. It includes drive control (turning the drive on and off), a closed-loop torque controller, software end-stops, signal logging and safety checks.

The goal of the torque controller is to command the actuator to exert a desired torque $\tau_{\text{des}}$ on its output shaft. The motor torque required for that, $\tau_{\text{des,mot}}$, is determined by a Disturbance Observer (DOB) [16], which is an improved version of the work described in [17] and [18]. The actual torque that the

joint exerts, $\tau_{act}$, is determined by measuring the deflection of the actuators' spring.

The joint is velocity-limited by a damping controller, which limits the commanded torque to the motor as $\tau_{limited,mot} = \min[\tau_{des,mot}, -D \cdot (v - v_{max})]$. Software end stops are based on the 'PVA limiter' as described in [19]. The end stops were implemented by making the maximum velocity $v_{max}$ dependent on the joint position $\varphi$ as $v_{max}(\varphi) = \sqrt{2\,a_{max}(\varphi - \varphi_{endstop})}$. This ensures constant deceleration (with $a = -a_{max}$) behavior close to the end stops. Beyond the end stop ($\varphi > \varphi_{endstop}$), $v_{max}$ becomes negative to escape from the region if it was accidentally entered. The main advantage of this software end stop algorithm over the conventional spring-damper implementation is that the commanded torque to the motor stays within reasonable values, even when approaching the end stop with high velocity. Still, the end stop feels very stiff for low velocities. Also, the penetration depth beyond the end stop does not depend on the approaching velocity (and is, theoretically, zero), and it does not suffer from the 'sticky effect'.

The end stop behavior takes precedence over the torque control. Therefore, close to the end stop (and also close to the maximum allowed velocity), the torque tracking of the joint may seem poor, but this is because it is more important to adhere to the end stops (or maximum velocity) to guarantee safety and to prevent damage to the device than to track the desired torque well.

## B. High-Level Control

On top of the low-level controller, a high-level controller needs to be implemented, which determines how much torque should be exerted on each of the joints. In order to facilitate different experiments with the exoskeleton, the high-level controller was implemented as a separate Simulink model which, after compilation, runs in TwinCAT next to the low-level controller. Communication between the two was handled by the TwinCAT ADS server. For each experiment, a separate Simulink model was developed and loaded into TwinCAT.

*1) The Neuromuscular Controller for Incomplete SCI Test Pilots:* The neuromuscular controller (NMC) was based on a sagittal-plane (2D), reflex-based simulation model developed by Geyer and Herr [4] and its 3D extension [5] (Figure 3). The sagittal model is actuated by seven Hill-type muscles per leg to control the ankle, knee, and hip, including the tibialis anterior, soleus, gastrocnemius, vasti, hamstring, gluteus maximus, and hip flexors. The 3D model includes four additional muscles — biceps femoris short head, rectus femoris, hip abductors, and hip adductors. Locomotion is produced by simple reflex rules, which engage depending on whether the leg is in stance or swing. During stance, the reflexes serve to provide weight support and to build positive force feedback to prepare for push-off. During swing, the reflexes utilize flexor muscles to allow the leg to swing forward and clear the ground. The neuro-muscular model achieves reasonable predictions of human gait characteristics such as joint kinematics, kinetic measures, and muscle activations [4]. It is also robust against perturbations and environmental disturbances in simulation [5]. Controller
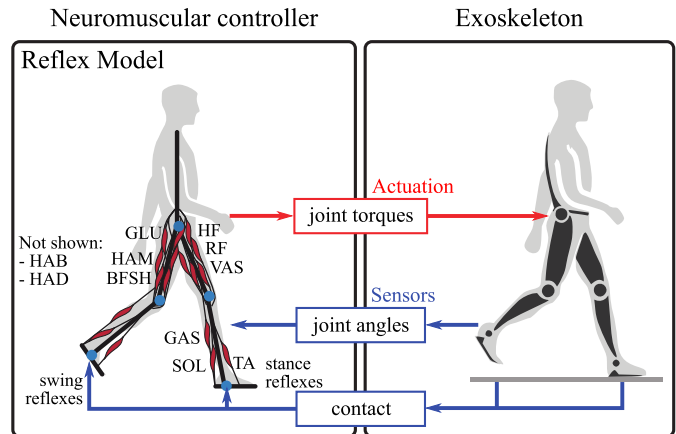


Fig. 3. Overview of wearable exoskeleton controlled by the NMC. The NMC uses joint kinematics and foot contact measurements to command joint torques to the device. Stance and swing reflexes are activated based on contact information.The muscles in the model are tibialis anterior (TA), soleus (SOL), gastrocnemius (GAS), vasti (VAS), hamstring (HF), gluteus maximus (GLU), hip flexors (HF), biceps femoris short head (BFSH), rectus femoris (RF), hip abductors (HAB), and hip adductors (HAD).

versions of the model have previously been implemented and evaluated on lower limb prostheses [20] and on assistive devices [6], [8], [21] with promising results for restoring walking function for impaired individuals.

Internally, the NMC consists of multiple muscle reflex control modules; each of which acts on one or more joints [6]. For the modular exoskeleton, this is an advantage because it can easily be tailored for the different configurations by activating only those modules for the joints used. For instance, for incomplete SCI test pilots having sufficient hip control, only the sagittal ankle and knee reflex modules were activated — modules governing hip movement were excluded. The NMC reacts to the movements of the thighs, resulting in a synchronized and natural gait. The NMC is nominally set to provide joint torques for a human simulation model to walk at 1.3 m/s but can be modified to address specific SCI test pilot needs. Controller gains, given as a percentage from zero to hundred percent, modify these nominal torques. Zero gain reduces to minimal impedance mode (a condition in which the robot seconds user's intention without delivering any assistive torques). At the broadest level, controller gains can be applied symmetrically (to both left and right legs) or asymmetrically. Joint level gains can also be modified to augment or reduce the level of assistance at each joint (e.g. the soleus and tibialis anterior for the ankle). Additionally, each muscle may be modified individually. For example, the soleus can be modified separately to yield the level of plantarflexion needed. A graphic user interface was set up to provide easy control and modification of controller settings.

*2) Combined Trajectory Controller and NMC for Complete SCI Test Pilots:* Whereas NMC might be very well suited for individuals with incomplete lesions, the implementation for individuals with complete lesions faces some challenges. First, initiating gait from stand still cannot yet be appropriately modelled with NMC. Second, NMC does not directly control joint trajectories, which could result in potential unsafe trajectories. In order to overcome these challenges for complete
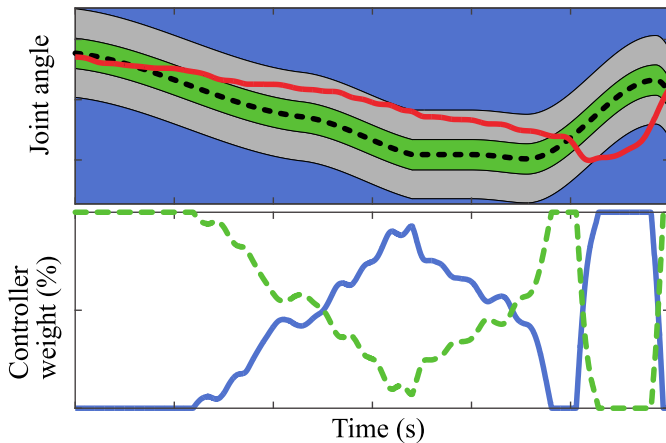
Fig. 4. The top panel visualises the concept of the combined NMC and trajectory controller in which the amount of deviation of the actual joint angle (red solid line) from the reference joint angle (dashed black line) determines whether the NMC controller (green region), the trajectory controller (blue region), or a weighted combination of both (grey area) is active. In the bottom panel, the relative weighs of the NMC controller (dashed green line) and trajectory controller (blue solid line) are shown for this example.

TABLE IV
SCI TEST PILOT EPIDEMIOLOGICAL DATA (BOTH HKA AND KA CONFIGURATION)

| Test Pilot | Age (years) | Lesion Time | AIS[1] Level | Lesion Level | Exo configuration |
|---|---|---|---|---|---|
| S1 | 30 | 5 years 6 months | A | D9 | HKA |
| S2 | 69 | 1 year 9 months | D | T10-T11 | KA |
| S3 | 47 | 1 year 1 month | D | L4-S3 | KA |

[1]American Spinal Injury Association Impairment Scale.

(Table IV; Figure 1 left). The incomplete test pilots (S2 and S3) used the knee-ankle (KA) configuration of the exoskeleton, controlled by the NMC. The NMC gains were pre-defined; the tuning was based on pilot experiments to simultaneously assess performance and perceived usability. We compared NMC gait to their shod gait (free walking without wearing the device). We evaluated the biomechanical gait changes, such as walking speed, joint kinematics, and joint torques from walking with the NMC-controlled exoskeleton. For gait analysis for shod conditions, joint angles and torques were retrieved based on motion capture data (OptiTrack, NaturalPoint, Corvallis, OR, recorded at 120 Hz) and ground reaction force data (BTS Bioengineering, Milan, Italy, recorded at 500 Hz) through inverse kinematics and dynamics (Opensim [22]). We evaluated the exoskeleton-assisted and shod joint angles and torques through qualitative comparisons with healthy gait patterns at a slow speed of 0.6 m/s (Fig. 7). The healthy data was derived from the average across eight healthy individuals walking on a treadmill [23].

The complete SCI test pilot (S1) used the hip-knee-ankle (HKA) configuration. Because the complete SCI test pilot was not able to walk without the exoskeleton, we only show results of the NMC combined with the trajectory controller. S1 was also supported by the FLOAT (Lutz Medical Engineering, Rüdlingen, Switzerland), a body weight support system that allows overground walking in a rectangular workspace and safe intervention in case of falls [24].

All SCI test pilots used crutches during the experiments and gave their informed consent for participation in the experiments and publication of photos with their image. The experiments were performed with approval of local ethics committee, the Comitato Etico Indipendente of Fondazione Santa Lucia, under approval reference CE/GROG.509.

SCI test pilots, the NMC was combined with an impedance based trajectory controller. The hip and knee joints were fully trajectory controlled with a speed-dependent reference joint trajectory generation algorithm based on the work by Koopman *et al.* [13]. The algorithm by Koopman generates reference joint trajectories for continuous walking. For usage in the exoskeleton, it was adapted to pause after each step so that the user can shift their weight and adapt their posture to be ready for the next step. By pressing a button integrated in the crutch handle, the user could initiate a step that moves one foot for the other to step or keep on walking, or a step that put one foot next to the other to end in standing posture.

The ankle joints were controlled by a combination of NMC and trajectory control (Figure 4): when the joint angle is close to the reference joint angle as dictated by the (above mentioned) reference joint trajectory (i.e., within a 'tunnel' around the reference trajectory), the NMC is in full control and the trajectory controller is switched off. When the joint angle deviates too much from the reference joint angle, the trajectory controller (a proportional-derivative or PD controller to reduce the error between actual joint angle and reference joint trajectory) gradually takes over to make sure that the deviation can be limited. This results in natural, NMC-governed behavior and trajectory-governed behavior if the ankle makes unexpected movements. Note that the software also allows this combination of NMC and trajectory control for the knee and hip joint, but this option was not tested on the SCI test pilots.

For the combined NMC-trajectory controller, the stiffness and damping of the trajectory controller and its tunnel width can be adjusted with the GUI (default: 750 Nm/rad; slightly overdamped).

## V. PRELIMINARY EVALUATION WITH SCI TEST PILOTS

Walking tests with the exoskeleton were performed by SCI test pilots with incomplete and complete spinal cord injury

## VI. RESULTS

This section shows the results of the experiments described in the previous section. We will show improvements in walking speed of the SCI test pilots and the joint kinematics and kinetics during experiments. But first we will show the accuracy of the low-level torque tracking since this is a prerequisite for impedance and NMC controllers.

### A. Torque Tracking

The high-level controller commands desired torques to the low-level controller, which should then track these torques as closely as possible. We define torque tracking error as the
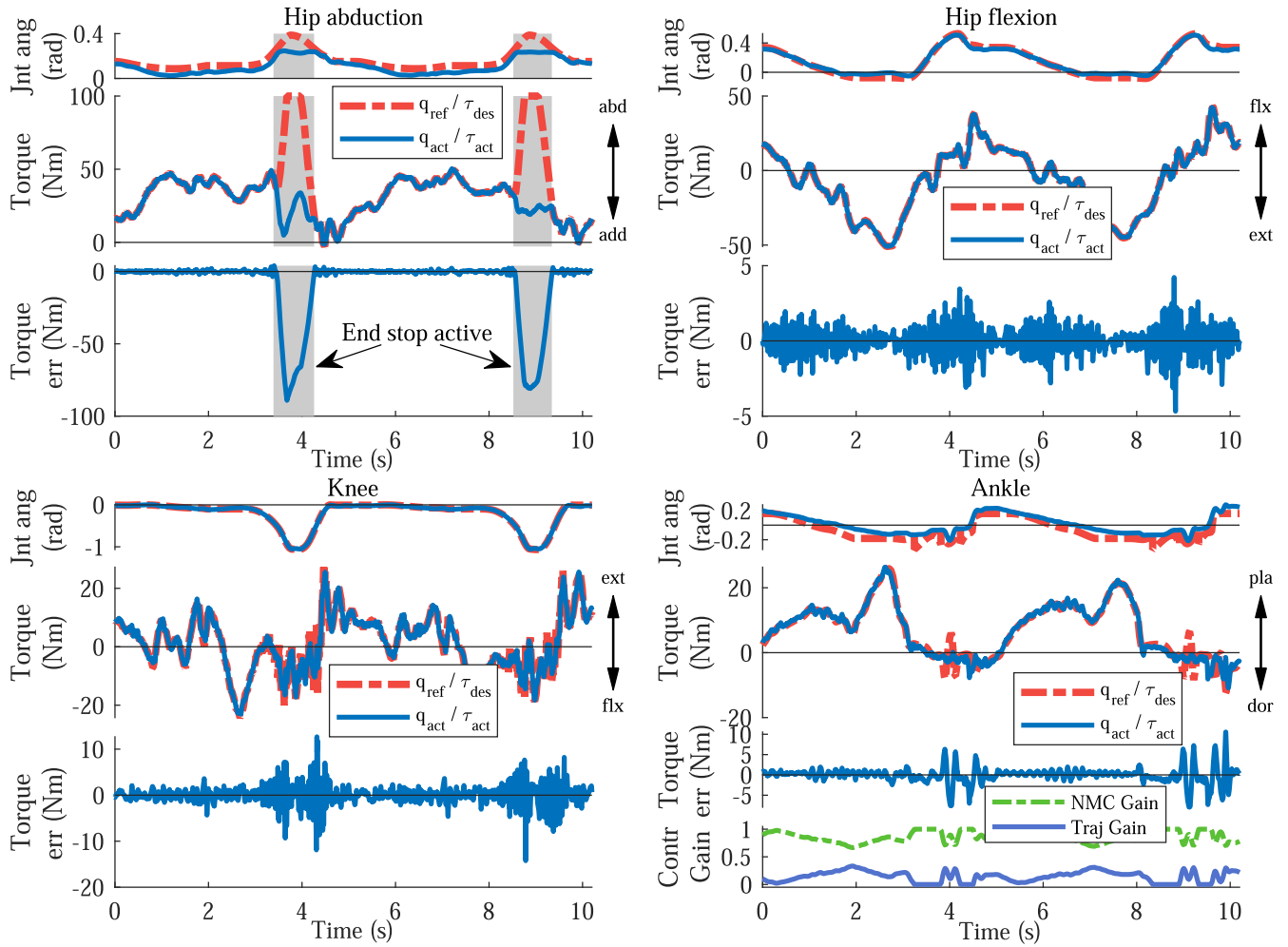
Fig. 5. Times series for the joint angle, the actual and desired torques and the torque error of the right leg for two typical strides of complete SCI test pilot S1. The grey areas indicate the time period in which a joint limiter was active.

measured actual torque $\tau_{act}$ minus the commanded torque $\tau_{des}$. Figure 5 shows the torque tracking of two typical strides of complete SCI test pilot S1. For this test pilot the root mean square tracking error (RMSE) when the software end-stop was not active was 0.6, 0.7, 1.4, and 1.8 Nm for the hip abduction/adduction, hip flexion/extension, knee flexion/extension, and ankle plantar/dorsal flexion, respectively.

By design, sometimes the torque tracking error could be large. This occurs when the joint nears the software end stop. Then the end stop controller, which minimizes the penetration beyond end stop, takes precedence over the torque tracking goal (which minimizes torque error). In Figure 5 the hip abduction angle approaches its maximal value and so is limited in two epochs, which is clearly reflected in the drastic increase of the torque error.

## B. Complete SCI Test Pilot

For S1, the complete SCI test pilot was able to walk with the combined NMC and trajectory controller with an average speed of 0.1 m/s (Table V.) Torques exerted by the exoskeleton are shown in Figure 5. The joint angles of the hip and knee tracked the reference joint angles reasonably

well when the software end-stop were not active. Ankle joint angles were not very well tracked since the NMC controller was relatively more active than the trajectory controller. We also collected data after the Symbitron project ended from a complete SCI individual completing all tasks of the Cybathlon competition, mostly without body weight support. In the Supplementary materials, videos and joint angles and torques from the exoskeleton can be found for standing up and down and for walking while crossing a tilted path, up and down stairs and ramps, opening and closing a door, slaloming through poles, and stepping over stones.

## C. Incomplete SCI Test Pilots

When used in KA configuration (incomplete SCI pilots S2 and S3), the NMC-controlled wearable exoskeleton could support a wide range of walking speeds for each SCI test pilot (Table V). The pilots were able to dictate the walking speed by varying their (still intact) thigh behavior; the NMC automatically adjusted the knee and ankle behavior accordingly.

Both test pilots walked faster with the aid of the robot than without it. The NMC allowed the SCI test pilots to change their walking speed and stride length. The individual's

TABLE V
RANGE OF WALKING SPEEDS

| SCI Test Pilot | Condition | Exo configuration | Speed (m/s) | | |
|---|---|---|---|---|---|
| | | | Min | Mean±s.d. | Max |
| S1 (AIS A) | Shod | – | – | – | – |
| | Exo | HKA | 0.06 | 0.10±0.03 | 0.16 |
| S2 (AIS D) | Shod | – | 0.25 | 0.33±0.05 | 0.40 |
| | Exo | KA | 0.23 | 0.61±0.12 | 0.76 |
| S3 (AIS D) | Shod | – | 0.41 | 0.50±0.07 | 0.61 |
| | Exo | KA | 0.54 | 0.87±0.15 | 1.05 |

For S2 and S3, strides with stride times $t < 0.8$ s and $t > 3$ s and speeds $< 0.2$ m/s were discarded to avoid any turning or very small steps at the beginning or end of trials. s.d.: standard deviation.
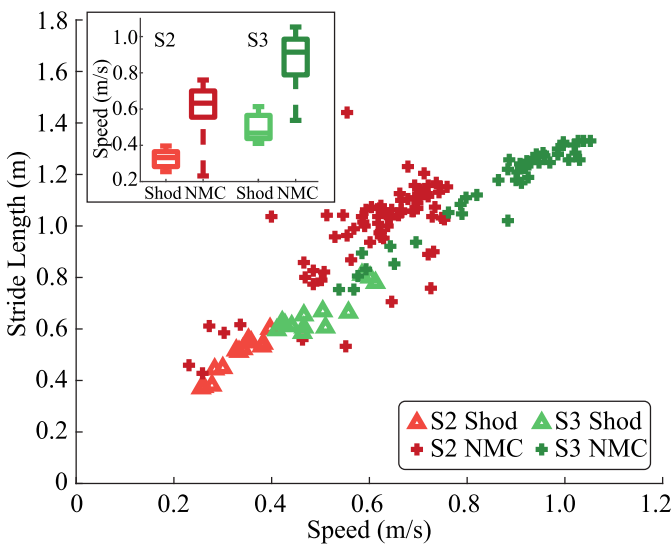


Fig. 6. Speed and stride length for S2 and S3 for the shod (triangle) and NMC (plus) conditions. Inset: boxplot of walking speeds for S2 and S3. The middle line in the box is the median speed while the bottom and top edges represent the 25th and 75th percentile, respectively. The whiskers extend to the minimum and maximum speeds. Strides with stride times $t < 0.8$ s and $t > 3$ s and speeds $< 0.2$ m/s were discarded to avoid any turning or very small steps at the beginning or end of trials.

stride length increased with speed (Figure 6). Incomplete SCI test pilot-specific NMC parameters were kept constant during all trials, and the NMC successfully supported variations in walking speed within and among each test pilot without any pre-defined trajectories.

NMC provided incomplete SCI test pilots with supporting torques that resulted in joint kinematics and kinetics that were similar to healthy gait (Figure 7). Healthy data at a walking speed of 0.6 m/s was used for qualitative comparisons [23]. Similar to healthy profiles, the NMC provided both complete SCI test pilots with a peak ankle plantarflexion torque to assist in ankle push-off and knee extension and flexion torques during stance. Without the exoskeleton, both S2 and S3 walked with a more dorsiflexed ankle angle. With the NMC, the ankle angles of both test pilots were less dorsiflexed and closer to normative ankle patterns. For S2, knee angles with NMC were similar in profile with shod condition and healthy data but with less knee flexion during swing. For S3, the knee torque
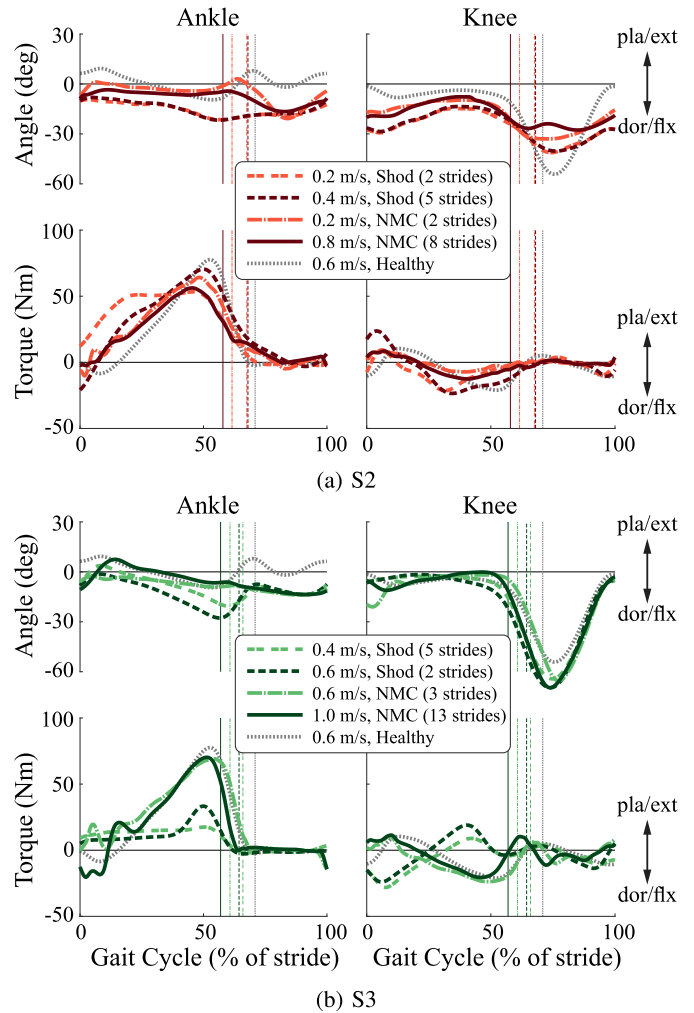


Fig. 7. Mean joint angles and torques for the right ankle and right knee for S2 and S3 as a function of stride. Walking conditions include shod (dashed or double-dashed) and NMC (solid or solid-dotted) with two different speeds (fast: dark, slow: light). Data from healthy persons (dotted) are included for comparison. Heel-strike at 0%; vertical lines indicate toe-off. Legend indicates the number of strides over which the mean was taken.

profiles with and without robotic assistance were different, but the NMC-provided torques were closer to natural healthy torque patterns with extension during the early part of stance and flexion in late stance. S3's own knee torques during stance could arise from the lack of knee flexion during stance.

Differing methods for recording kinematics and determining joint torques could account for some of the disparities between shod and NMC conditions. For the NMC conditions, exoskeleton ankle and knee angles and torques were measured from the wearable exoskeleton encoders and torque sensors. For the shod conditions, human joint angles and torques were retrieved based on motion capture data through inverse kinematics and dynamics. In particular, the NMC torque is the external torque exerted by the exoskeleton while the shod torque is the net joint torque based on a rigid body model through standard inverse dynamics calculations.

## VII. DISCUSSION

Our aim was to develop an exoskeleton for individuals with a SCI that can be personalized to a broader range of

lesion levels and gradations. We have developed a modular system that can be customized for each person by selecting the relevant joint modules and by adjusting the 23 length settings appropriately.

Experiments were done with different configurations: HKA (Hip/Knee/Ankle) and KA (Knee/Ankle) on test pilots with different impairment levels. For people who still had remaining walking ability , we found an increased walking speed when wearing the exoskeleton. The NMC controller enabled the exoskeleton to automatically adapt to changes in walking velocity. The emerging gait and torques were mostly similar to those found in healthy people. People who fully lost their walking ability could also walk again when wearing the exoskeleton.

We conclude from these preliminary results that the NMC can support gait for a large range of speeds and is capable of generating healthy-like gait for SCI test pilots with various levels of mobility during overground walking. In particular, for S2 and S3, NMC ankle and knee torque profiles were similar to healthy ones. While there were some differences in joint angles, the NMC produced more normative ankle angles than the SCI test pilots could achieve without the aid of the exoskeleton. Using only a fixed set of controller gains tailored to each user's needs, the diversity of gaits achieved demonstrates the versatility and capability of a bio-inspired controller. The modularity of this controller is also particularly suitable for use in a modular exoskeleton, such as the one detailed in this paper. From the results we presented and data in the supplementary materials, it is evident that for the incomplete SCI test pilots all requirements were met, while for complete SCI test pilots all mandatory requirements were achieved (see Table I).

In addition to the experiments presented in this paper, we also used the exoskeleton to support standing balance in our SCI test pilots [25]. Using the exoskeleton in the ankle-knee configuration, we tested how various low-level controllers (PD control on center of mass and a momentum-based controller [26]) performed in assisting individuals with incomplete SCI with maintaining their balance while standing. The centre of mass was estimated from the joint angles of the exoskeleton and IMUs attached to the chest and right thigh. Results were promising since all SCI test pilots improved their balance recovery after being perturbed. One of the SCI test pilots could only stand stably with help of the exoskeleton [25].

### A. Comparison to Other Exoskeletons

In Table VI, the main characteristics are shown for some exoskeletons. Care should be taken with comparisons because the exoskeletons have been developed for different purposes (e.g., commercial/home usage vs research), therefore large differences are to be expected. The Symbitron exoskeleton is heavier due the higher number of actuators. The exception is the Atalante exoskeleton with 12 actuated degrees of freedom. With this exoskeleton, complete SCI individuals were able to walk slowly at 0.1 m/s without using crutches. Other devices do (mainly) use direct actuation, while we employ SEA. The

#### TABLE VI
COMPARISON OF MAIN CHARACTERISTICS FOR VARIOUS EXOSKELETONS*

| | Mass (kg) | Powered DOFs | Operation time (h) | Actuation principle |
|---|---|---|---|---|
| Symbitron | 37.2 | 8 (HF, HA, KF, AP) | 1 | SEA (all) |
| Mina V2 | 34 | 6 (HF, KF, AP) | 2.5 | Direct |
| Twiice | 15 | 4 (HF, KF) | 2-3 | Direct |
| Rewalk | 23.3 | 4 (HF, KF) | 2.40** | Direct |
| Ekso | 20 | 4 (HF, KF) | 4 | Direct |
| Indego | 12 | 4 (HF, KF) | 4 | Direct |
| Varileg | 35 | 4 (HF, KF) | 1.5-2 | SEA (knee) |
| Alalante | 59 | 12 (HF, HA, HR, KF, AP, AE) | 3 h | direct |

* Most recent data retrieved from the available literature
** Continuous walking.

advantage of using SEA is to have much better force control capacity, which is essential for implementing bio-inspired controllers and for partial support of gait and balance. Most lower-leg exoskeletons for SCI do not actuate the ankle, while we do. An ankle-only exoskeleton evaluated in individuals with SCI showed improved push off kinematics and a small reduction of activity in muscles involved in push off [27]. We recently found similar advantages of such a device [7]. IHMC's Mina v2 exoskeleton [28] also includes actuation of the ankle. In their report about IHMC's participation in the Cybathlon 2016, the authors state that the addition of the powered ankle to Mina v2 indeed propelled the patient forward during walking and made walking more stable. Also, in the Atalante exoskeleton, active control of the ankle is necessary to maintain balance. So, inclusion of ankle actuation holds promise to improve walking efficiency in individuals with SCI and is essential to include for supporting balance.

### B. Future Work

Future development for the exoskeleton will be aimed at reducing weight, increasing robustness, and increasing maintainability and further developing high level control software.

Weight reduction was a major goal in design of the actuators. The structure, however, was harder to optimize due to the many available size-adjustments of the exoskeleton. Additionally, its modularity needs to be reconsidered because it increases the number of interfaces even further. Future development will be aimed at finding fast and low-cost ways to produce a one-to-one structure for each SCI test pilot to minimize mass and volume. Also the weight of the backpack will be reduced significantly.

Large sources of failure in the exoskeleton were the cables and connectors. Again, because of the number of available size adjustments, the cables were running external to the exoskeleton structure, creating vulnerabilities. Here, modularity also creates additional complexity by demanding an additional connection and requiring variable cable length. More effort needs to be made in the integration of the cables and connectors in the structure. Finally, design for maintenance was greatly underestimated in the project. In future designs, electronics should be accessible and easily replaced.

To improve the functionality of the exoskeleton, we will also improve the high level controller to support balance during

walking to reduce the reliance on crutches for complete SCI individuals when wearing the exoskeleton. We are also developing a flexible path planner such that the exoskeleton can cope with more challenging environments, such as those used in the Cybathlon competition. While our future improvements will further advance exoskeleton performance and usability, the Symbitron exoskeleton shown here demonstrates that tailored assistance through modularity in hardware and control is promising for restoring the gait of individuals with a spinal cord injury, whether they required targeted aid or full support.

## ACKNOWLEDGMENT

## REFERENCES

[1] A. Young and D. Ferris, "State of the art and future directions for lower limb robotic exoskeletons," *IEEE Trans. Neural Syst. Rehabil. Eng.*, vol. 25, no. 2, pp. 171–182, Mar. 2016.

[2] M. W. M. Post *et al.*, "Progress of the Dutch spinal cord injury database: Completeness of database and profile of patients admitted for inpatient rehabilitation in 2015," *Topics Spinal Cord Injury Rehabil.*, vol. 24, no. 2, pp. 141–150, Mar. 2018.

[3] F. M. Maynard *et al.*, "International standards for neurological and functional classification of spinal cord injury," *Amer. Spinal Injury Assoc.*, vol. 35, pp. 266–274, May 1997.

[4] H. Geyer and H. Herr, "A muscle-reflex model that encodes principles of legged mechanics produces human walking dynamics and muscle activities," *IEEE Trans. Neural Syst. Rehabil. Eng.*, vol. 18, no. 3, pp. 263–273, Jun. 2010.

[5] S. Song and H. Geyer, "A neural circuitry that emphasizes spinal feedback generates diverse behaviours of human locomotion," *J. Physiol.*, vol. 593, no. 16, pp. 3493–3511, Aug. 2015.

[6] F. Dzeladini *et al.*, "Effects of a neuromuscular controller on a powered ankle exoskeleton during human walking," in *Proc. 6th IEEE Int. Conf. Biomed. Robot. Biomechatronics (BioRob)*, Jun. 2016, pp. 617–622.

[7] F. Tamburella *et al.*, "Neuromuscular controller embedded in a powered ankle exoskeleton: Effects on gait, clinical features and subjective perspective of incomplete spinal cord injured subjects," *IEEE Trans. Neural Syst. Rehabil. Eng.*, vol. 28, no. 5, pp. 1157–1167, May 2020.

[8] A. R. Wu *et al.*, "An adaptive neuromuscular controller for assistive lower-limb exoskeletons: A preliminary study on subjects with spinal cord injury," *Frontiers Neurorobotics*, vol. 11, p. 24, Jun. 2017.

[9] C. Meijneke, S. Wang, V. Sluiter, and H. van der Kooij, "Introducing a modular, personalized exoskeleton for ankle and knee support of individuals with a spinal cord injury," in *Wearable Robotics: Challenges and Trends*, J. González-Vargas, J. Ibáñez, J. L. Contreras-Vidal, H. van der Kooij, and J. L. Pons, Eds. Cham, Switzerland: Springer, 2017, pp. 169–173.

[10] M. E. Roebroeck, C. A. M. Doorenbosch, J. Harlaar, R. Jacobs, and G. J. Lankhorst, "Biomechanics and muscular activity during sit-to-stand transfer," *Clin. Biomechanics*, vol. 9, no. 4, pp. 235–244, Jul. 1994.

[11] S. R. Chang, R. Kobetic, and R. J. Triolo, "Understanding stand-to-sit maneuver: Implications for motor system neuroprostheses after paralysis," *J. Rehabil. Res. Develop.*, vol. 51, no. 9, pp. 1339–1352, 2014.

[12] J. L. Lelas, G. J. Merriman, P. O. Riley, and D. C. Kerrigan, "Predicting peak kinematic and kinetic parameters from gait speed," *Gait Posture*, vol. 17, no. 2, pp. 106–112, Apr. 2003.

[13] B. Koopman, E. H. F. van Asseldonk, and H. van der Kooij, "Speed-dependent reference joint trajectory generation for robotic gait support," *J. Biomechanics*, vol. 47, no. 6, pp. 1447–1458, Apr. 2014.

[14] A. N. Lay, C. J. Hass, and R. J. Gregor, "The effects of sloped surfaces on locomotion: A kinematic and kinetic analysis," *J. Biomechanics*, vol. 39, no. 9, pp. 1621–1628, Jan. 2006.

[15] S. Nadeau, B. J. McFadyen, and F. Malouin, "Frontal and sagittal plane analyses of the stair climbing task in healthy adults aged over 40 years: What are the challenges compared to level walking?" *Clin. Biomechanics*, vol. 18, no. 10, pp. 950–959, Dec. 2003.

[16] W. F. Rampeltshammer, A. Q. L. Keemink, and H. van der Kooij, "An improved force controller with low and passive apparent impedance for series elastic actuators," *IEEE/ASME Trans. Mechatronics*, vol. 25, no. 3, pp. 1220–1230, Jun. 2020.

[17] N. Paine *et al.*, "Actuator control for the NASA-JSC Valkyrie humanoid robot: A decoupled dynamics approach for torque control of series elastic robots," *J. Field Robot.*, vol. 32, no. 3, pp. 378–396, May 2015.

[18] K. Kong and M. Tomizuka, "Nominal model manipulation for enhancement of stability robustness for disturbance observer-based control systems," *Int. J. Control, Autom. Syst.*, vol. 11, no. 1, pp. 12–20, Feb. 2013.

[19] J. Meuleman, E. van Asseldonk, G. van Oort, H. Rietman, and H. van der Kooij, "LOPES II—Design and evaluation of an admittance controlled gait training robot with shadow-leg approach," *IEEE Trans. Neural Syst. Rehabil. Eng.*, vol. 24, no. 3, pp. 352–363, Mar. 2016.

[20] M. F. Eilenberg, H. Geyer, and H. Herr, "Control of a powered ankle–foot prosthesis based on a neuromuscular model," *IEEE Trans. Neural Syst. Rehabil. Eng.*, vol. 18, no. 2, pp. 164–173, Apr. 2010.

[21] V. R. Garate *et al.*, "Walking assistance using artificial primitives: A novel bioinspired framework using motor primitives for locomotion assistance through a wearable cooperative exoskeleton," *IEEE Robot. Autom. Mag.*, vol. 23, no. 1, pp. 83–95, Mar. 2016.

[22] S. L. Delp *et al.*, "OpenSim: Open-source software to create and analyze dynamic simulations of movement," *IEEE Trans. Biomed. Eng.*, vol. 54, no. 11, pp. 1940–1950, Nov. 2007.

[23] A. R. Wu, C. S. Simpson, E. H. F. van Asseldonk, H. van der Kooij, and A. J. Ijspeert, "Mechanics of very slow human walking," *Sci. Rep.*, vol. 9, no. 1, pp. 1–10, Dec. 2019.

[24] H. Vallery *et al.*, "Multidirectional transparent support for overground gait training," in *Proc. IEEE 13th Int. Conf. Rehabil. Robot. (ICORR)*, Jun. 2013, Art. no. 6650512.

[25] A. Emmens *et al.*, "Improving the standing balance of paraplegics through the use of a wearable exoskeleton," in *Proc. 7th IEEE Int. Conf. Biomed. Robot. Biomechatronics (Biorob)*, Aug. 2018, pp. 707–712.

[26] D. E. Orin and A. Goswami, "Centroidal momentum matrix of a humanoid robot: Structure and properties," in *Proc. IEEE/RSJ Int. Conf. Intell. Robots Syst.*, Sep. 2008, pp. 653–659.

[27] G. S. Sawicki, A. Domingo, and D. P. Ferris, "The effects of powered ankle-foot orthoses on joint kinematics and muscle activation during walking in individuals with incomplete spinal cord injury," *J. NeuroEng. Rehabil.*, vol. 3, no. 1, p. 3, 2006.

[28] R. Griffin *et al.*, "Stepping forward with exoskeletons: Team IHMC? s design and approach in the 2016 cybathlon," *IEEE Robot. Autom. Mag.*, vol. 24, no. 4, pp. 66–74, Dec. 2017.